Reconstruction with criterion from labeled markers: new approach based on the morphological watershed

Damián Vargas-Vázquez
Universidad Autonóma de Querétaro
Facultad de Ingeniería
76010 Centro Universitario
Querétaro, Mexico
E-mail: damianvv@uaq.mx

Jose Crespo
Victor Maojo
Universidad Politécnica de Madrid
GIB–LIA Departamento LSIIS
and
Departamento IA Facultad de Informática
28660 Boadilla del Monte
Madrid, Spain

Jose Gabriel Ríos-Moreno
Mario Trejo-Perea
Universidad Autonóma de Querétaro
Facultad de Ingeniería
76010 Centro Universitario
Querétaro, Mexico

Abstract. *The goal of image segmentation is to partition an input image into a set of regions. In mathematical morphology, the reconstruction of images from markers has proven to be useful in morphological filtering and image segmentation. The utilization of a criterion in the problem of the image reconstruction from an image marker has been partially treated elsewhere. We further investigate this idea and extend it to the problem of image reconstruction from labeled markers by proposing a new method based on the "watershed" transformation as an alternative in image segmentation. The image gradient is considered as a topographic relief that is flooded (similarly as in a normal watershed). However, a criterion is added in this reconstruction process that enables the flexibility to separate structures of interest. Following the flooding analogy on topographic reliefs, this flooding process is limited to certain zones to control the recovering process of structures shapes. Experimental results are provided. A comparison with a viscous watershed is performed to show the differences between them. The technique is applied mainly in the biomedical domain, although the technique can generally be applied to other areas.*
 [DOI: 10.1117/1.3491494]

1 Introduction

The segmentation of an image into its significant regions is a key problem in image analysis. After the image segmentation process has been performed, it is possible to compute measures from the extracted regions and to analyze their adjacency relationships. For this reason, the segmentation process is a fundamental step in image data quantitative analysis.

Image segmentation is based on two fundamental principles: discontinuity and similarity. The edge-based segmentation is based on the first principle, whereas the region-based segmentation uses mainly the second principle.

For edge detection, it is assumed that image objects show small variations (in gray level or color), and that their edges are characterized by high variations in their neighborhood. Examples of these techniques are the first- or second-derivative operators, and some morphological operators. On the other hand, for the detection of regions, an analysis of homogeneous regions is performed. Some of the most widely used region-based techniques are binarization based on thresholds, region growth, region division, and similarity of textures, in color or gray level.[1,2]

Morphology mathematical (MM)[3–10] holds on a special place in image analysis and processing. MM techniques for image segmentation usually involve the usage of the so-called markers, which locate the input image significant regions.

The watershed transform[11–15] is a segmentation method that has been developed within the MM framework. This method shares some similarities with region growing techniques,[16–19] although it uses edge information in a distinctive way. The watershed transformation operates

Paper 09157R received Sep. 1, 2009; revised manuscript received Apr. 4, 2010; accepted for publication Aug. 11, 2010; published online Dec. 30, 2010

1017-9909/2010/19(4)/043001/15/$25.00 © 2010 SPIE and IS&T

on an input image that is considered as a topographical surface.

A wide variety of new proposals with different modifications have arisen from this transformation (e.g., topological watershed,[20] watersnakes,[21] viscous watershed[22]). Among these proposals, the viscous watershed is one of the most interesting, and it shares some similarities with the approach presented in this paper. It introduces a viscosity factor that modifies the way in which the forms are recovered. This viscosity is applied to the scenario and not to the markers in an individual manner.

On other hand, the use of reconstruction algorithms in MM has been successfully used in the stages of image processing and analysis. Filters by reconstruction[23–30] have become powerful tools that enable us to eliminate undesirable features without practically affecting desirable ones. These filters are computed by reconstructing a reference image f from a marker image g, and they preserve well the shapes of the marked structures.

A new type of transformations—known as transformation with a reconstruction criterion—is derived from filters by reconstruction. A modification of the reconstruction process, in particular the inclusion of a criterion, enables us to control the shape of some structures while preserving contours and the structures of interest. The main feature of these transformations is that they enable us to obtain intermediate results between the standard morphological opening (or respectively, closing) and the opening (respectively, closing) by reconstruction, and some of their inconveniences can be avoided.

In this paper, we propose a new segmentation technique based on the watershed transform that performs an image reconstruction process with criterion from labeled markers. The image is considered as a topographical surface that will be flooded (as in the traditional watershed transform). However, a criterion is added to the flooding process to attain a greater flexibility and to control how the image structures are recovered. Some preliminary results were presented in Ref. 31. Unlike the viscous watershed, our approach considers a modified flooding mechanism applied individually to each involved marker in the reconstruction process.

The paper is organized as follows. Section 2 briefly introduces some basic concepts of the transformation with reconstruction criterion. Section 3 describes some concepts of the watershed transform. Also, a variation of the watershed method (the so-called "viscous watershed") that is related to our approach is commented on in this section. The statement of the problem this paper addresses is discussed in Sec. 4. Section 5 introduces the main ideas behind our approach. We consider the problem of image reconstruction (with criterion) using labeled markers in both the binary and the gray-level case, highlighting the differences with the normal reconstruction (i.e., where no criterion is employed). In Sec. 6, the proposed strategy is discussed and is compared with the viscous flooding. Section 7 provides some results appertaining to the biomedical domain. Finally, conclusions are given in Sec. 8.

2 Openings and Closings with Reconstruction Criterion

Morphological filters are nonlinear transformations that modify geometric features of images. The basic morphological filters are the morphological opening and the morphological closing with a certain structuring element. In general, this structuring element is a set that describes a simple shape that probes an input image. These filters present several inconveniences in some situations. In general, if the undesirable features are eliminated, the remaining structures will be changed. On the other hand, filters by reconstruction have become powerful tools that enable us to eliminate undesirable features without necessarily affecting desirable ones.

From a practical point of view, filters by reconstruction are built by means of a reference image and a marker image. These filters enable the complete extraction of the marked objects while preserving edges. The openings (or, respectively, closings) with reconstruction criteria used in this paper enable us to obtain intermediate results between the morphological opening (or, respectively, closing) and the opening (respectively, closing) by reconstruction and to avoid some of their inconveniences.

These filters by reconstruction with criterion have been partially treated in Refs. 32–37. In this paper, we study the application of the reconstruction criterion to the problem of the reconstruction of an input image from labeled markers (or connected components).

The process to build these types of transformations involves the use of a reference image and a marker image as in the reconstruction case. Thus, a reconstruction process of a marker image inside a reference image is made (as is the case in reconstruction transformations), but a reconstruction criterion is taken into account.

Let f and g be the reference and marker images, respectively. We consider the next propagation criteria:

$$f \wedge \gamma_\lambda \delta(g) \quad \text{and} \quad f \vee \varphi_\lambda \varepsilon(g). \tag{1}$$

The first applies to openings, and the second, to closings. We refer in the following expressions only to the opening case (dual expressions apply also to the closing case).

Let us remember that, in the normal opening by reconstruction, the operation used is $f \wedge \delta(g)$.

In Eq. (1), the opening γ_λ plays the special role of a propagation criterion. We have the following inequality: $g < \gamma_\lambda(g) < \delta(g)$, where g is a marker image.

Using $g = \gamma_\mu(f)$ (for $\lambda \leq \mu + 1$) as a marker, the opening with reconstruction criterion $\hat{\gamma}_{\lambda,\mu}$ arises by iterating the operator $\sigma^1_{\lambda,f}\{\gamma_\mu(f) = f \wedge \gamma_\lambda \delta[\gamma_\mu(f)]\}$ until idempotence, i.e.,

$$\begin{aligned}\hat{\gamma}_{\lambda,\mu}(f) &= \lim_{n\to\alpha} \sigma^n_{\lambda,f}[\gamma_\mu(f)] \\ &= \underbrace{\sigma^1_{\lambda,f}\sigma^1_{\lambda,f}\ldots\sigma^1_{\lambda,f}[\gamma_\mu(f)]}_{\text{until idempotence}}.\end{aligned} \tag{2}$$

Note that as in the preceding expressions, an opening γ_μ is normally used to compute the marker image, and that leads to the compact notation of using the symbol $\hat{\gamma}_{\lambda,\mu}$ for an opening with reconstruction criterion where the marker image is $\gamma_\mu(f)$. Sometimes, however, another type of marker is desired, and we can use the $\hat{\gamma}_{\lambda,g}$ symbol to refer to an opening with reconstruction criterion, where g is a general marker image.

The openings and closings with the reconstruction criterion enable us to control the propagation of the reconstruction, and they compute outputs that are intermediate between

those obtained (1) by applying standard (nonconnected) morphological filters and (2) by connected morphological filters.

3 Watershed Concepts

In this section, we introduce some general concepts related with the watershed transform, which are useful to better understand the approach described in this paper.

3.1 *General Definitions*

We consider only digital images in the following. A gray-level image can be represented by a function $f : D \to L$, where D is a subset of Z^2, and L is a subset of Z (Z denotes an integer set).

A section of image f at level i (where $f : D \to L$) is a set $X_i(f)$ defined as $X_i(f) = \{x \in D : f(x) \geq i\}$. Let M be a set of D. For every point y of M, we assign the distance function of y to complementary set $C(M)$ as

$$\forall \gamma \in M, \quad d(y) = \text{dist}[y, C(M)], \tag{3}$$

where dist $[y, C(M)]$ is the shortest distance between y and one point of $C(M)$.

Let $X \subset D$ be a set, and let x and y denote two points of X. We define the geodesic distance $d_X(x,y)$ between x and y as the length of the shortest path (if any) included in X and linking x and y (Ref. 13).

Suppose now that M is composed of several connected components (markers) M_i. The geodesic zone of influence $z_X(M_i)$ of marker M_i is the set of points of X located at a finite geodesic distance from M_i that are closer to M_i than to any other marker M_j:

$$z_X(M_i) = \{x \in X : \text{d}x(x, M_i) \quad \text{finite}, \\ \forall j \neq i, \text{d}x(x, M_i) < \text{d}x(x, M_j)\}. \tag{4}$$

The boundaries between the influence zones constitute the geodesic skeleton by influence zones (SKIZ) of M in X. We can write

$$IZ_X(M) = \bigcup_i z_X(M_i) \tag{5}$$

and

$$\text{SKIZ}_X(M) = X \backslash IZ_X(M), \tag{6}$$

where $\backslash$ stands for the set subtraction.

3.2 *Watershed Transform*

A gray-level image can be represented as a topographical surface: the gray level of each pixel is the elevation at this point, and the basins and valleys of the relief correspond to the darkest zones. On the other hand, mountains and crests correspond to brighter zones.[12]

The image considered as a topographical surface is not the original image but its gradient (more specifically the gradient module of original image). The morphological gradient (like Beucher's gradient[12,38]) is an operator that approximates the derivative module; this operator emphasizes the pixel intensity variations within vicinity determined by a structuring element.

The watershed is normally computed using a flooding process. If holes are pierced in the topographical surface at the regional minima locations, and we progressively flood this surface using different water sources (starting from the minima of lower altitude), water flows following the surface relief. Dams are raised at the places where the waters of different minima meet so to prevent their mixture.

At the end of this flooding procedure, each minimum will be surrounded by dams that delineate their associated basins. The segmentation result using this transformation will be the separation line (or watershed) between different basins.

3.3 *Viscous Watershed*

This section discusses one variant of the watershed transform that introduces some shape restrictions and that is, therefore, related to the technique presented in this paper.

The viscous flooding concept was proposed by Meyer,[22] and it can be related to a geophysical analogy originally commented by Matheron when presenting the morphological opening.[39]

If we want to introduce a geometric restriction in segmentation algorithms based on the watershed, one possibility is to perform a flooding with a "viscous" fluid. Two possible alternatives exist. The first option consists of simulating a viscous flooding for the construction of the watershed line. The work in Refs. 40 and 41 follow this possibility. The second option is to modify the relief of the topographical surface, so that to flood this new relief with a nonviscous fluid produces a flooding progression similar to that of a viscous fluid over a nonmodified relief.[42–44]

The idea suggested in the "viscous watershed" consists in modifying the topology of the image gradient using a "viscous closing." Then, a traditional watershed transformation is applied to the filtered gradient. The advantage of this method is that we can apply the efficient and fast algorithms of the traditional watershed.

Viscosity can be dependent on the pressure (for fluids with physical characteristics like the mercury) or on the temperature (for fluids with physical characteristics like the oil). Depending on the model used (determined by the fluid characteristics) viscosity changes based on physical conditions.

Figure 1 shows, in a graphical way, the effect of a viscosity diminution on a surface. When the fluid becomes less viscous, the space that the fluid fills increases. Computationally, the fluid viscosity is determined by the relation that exists between the size of used structuring element and the related physical condition (i.e., pressure or temperature).

For practical purposes, in this paper we work with a fixed viscosity for all the flooding levels, so that the comparative with the proposed method will be more comprehensible.

4 Problem Statement and General Considerations

The problem addressed in this work is the following: To design a gradient flooding strategy in which a criterion is imposed at all levels and stages of the flooding. From the previous statement, it follows that the final segmented shapes also satisfy such criterion.

The implementation philosophy of our technique originated from a type of morphological filtering that utilizes a shape criterion. From the fact that the extracted shapes must satisfy some size and shape constraints, it ensures that it is possible that some groups of pixels are not flooded (i.e., they are not assigned to any catchment basin in the final segmentation). Note that, however, in practice the number of pixels

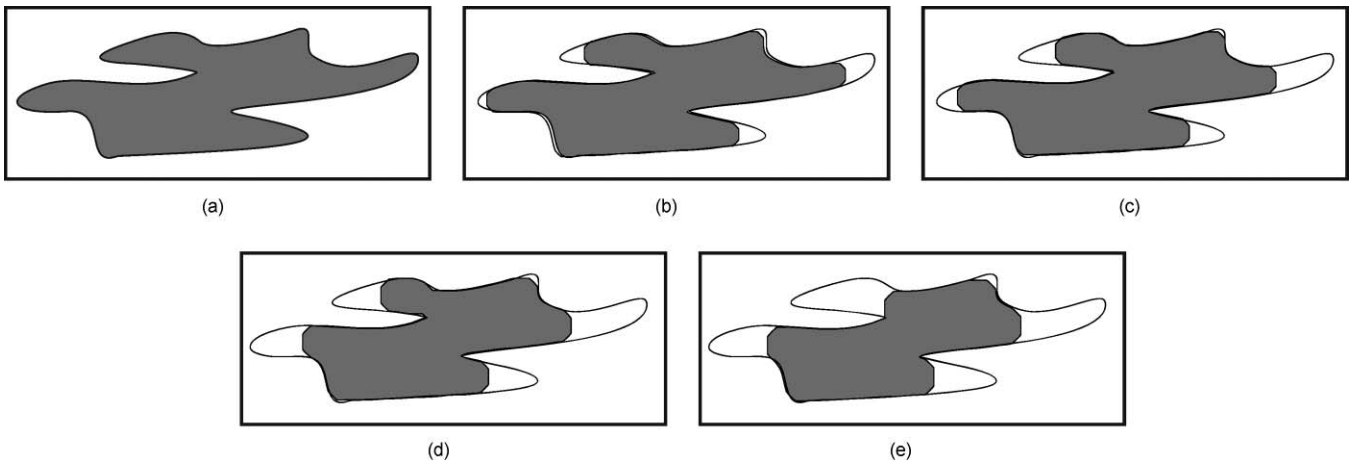

Fig. 1 (a) Flooding scenario with a non-viscous fluid; (b), (c), (d), (e) examples of lakes formed by fluids of increasing viscosity.

left unflooded is very small compared to the total number of image pixels.

For particle extraction situations (such as those often encountered in biomedical image analysis), it is usually unimportant that some pixels are not flooded (i.e., that they are left unassigned). It is important, on the other hand, that shapes satisfy certain constraints.

5 Reconstruction with Criterion from Labeled Markers: Binary Case: Binary Case

In this section, we discuss the addition and application of a criterion on the image reconstruction from labeled markers problem. The computation of the influence zones associated with markers, and the differences caused by the added criterion, are analyzed in the binary case. We also consider the possibility that arises in some situations when some pixels do not belong to any influence zone.

Later, these concepts are applied to gray-level images. A modified flooding process is proposed as an alternative for segmenting regions of interest; in this way, we are able to extract regions with additional flexibility.

Let $P_X(x,y)$ denote the set of paths that link x and y. Such a set can be the empty set, in particular if x and y belong to disjoint components of X. We can write the geodesic distance as

$$\mathrm{d}x(x,\,y) = \wedge\{\ell(r),\, r \in P_X(x,y)\}, \tag{7}$$

$$\mathrm{d}x(x,\,y) = \infty \quad \text{if} \quad P_X(x,y) = \Phi, \tag{8}$$

where ℓ is the length of the path of points (number of points, in a digitized space).

Let us suppose that we apply an opening with reconstruction criterion $\hat{\gamma}_{\lambda,g}$ (where g is the initial set of markers, i.e., $g = \bigcup_i M_i$) to image X. This affects the geodesic distance $\mathrm{d}x(x,\,y)$ in the expressions indicated above, and the following geodesic distance $D_X(x,\,y)$ relative to the filtered set must be used instead:

$$D_X(x,\,y) = \wedge\{\ell(r),\, r \in P_{\hat{\gamma}_{\lambda,g}(X)}(x,\,y)\}, \tag{9}$$

$$D_X(x,\,y) = \infty \quad \text{if} \quad P_{\hat{\gamma}_{\lambda,g}(X)}(x,\,y) = \Phi. \tag{10}$$

Note that, instead of paths included in X, we are considering paths included in the filter output $\hat{\gamma}_{\lambda,g}\,(X)$.

Figure 2 illustrates the $D_X(x,\,y)$ concept. Figures 2(a) and 2(b) display the usual case and the shortest path between a pair of points x and y that belong to X. Figure 2(c) visualizes the filter output $\hat{\gamma}_{\lambda,g}\,(X)$, and Fig. 2(d) displays the shortest path between x and y that is included in $\hat{\gamma}_{\lambda,g}\,(X)$. Note that $\mathrm{d}x(x,y)$ is quite different from $D_X(x,y)$ in this example.

We now consider the problem of computing the influence zones associated to a set of markers. The following expression will define the new $\hat{z}_X(M_i)$ influence zone of marker M_i:

$$\hat{z}_X(M_i) = \{x \in \hat{\gamma}_{\lambda,g}(X)\colon D_X(x,\,M_i) \quad \text{finite},$$
$$\forall j \neq i,\, D_X(x,\,M_i) < D_X(x,\,M_j)\}. \tag{11}$$

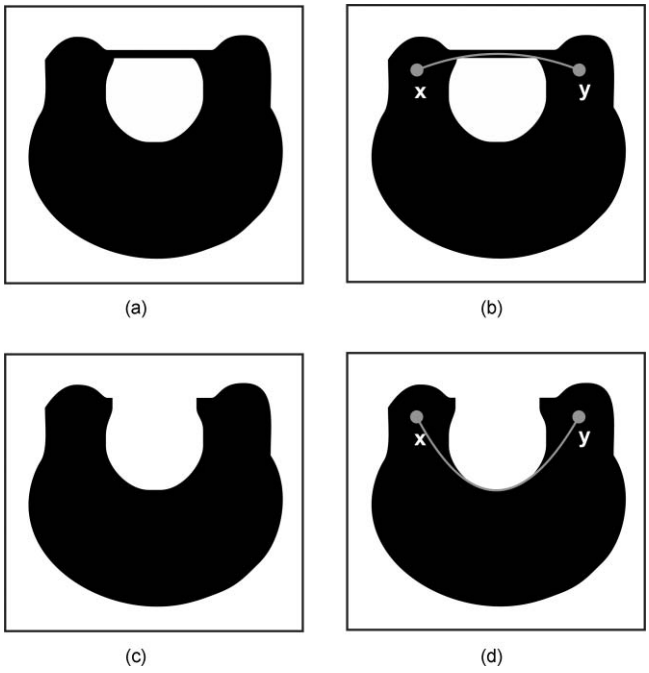

Fig. 2 Differences regarding the shortest path: (a) Original image X; (b) shortest path between a pair of points x and y that belong to X; (c) filter output $\hat{\gamma}_{\lambda,g}\,(X)$; (d) shortest path between x and y that is included in $\hat{\gamma}_{\lambda,g}\,(X)$.

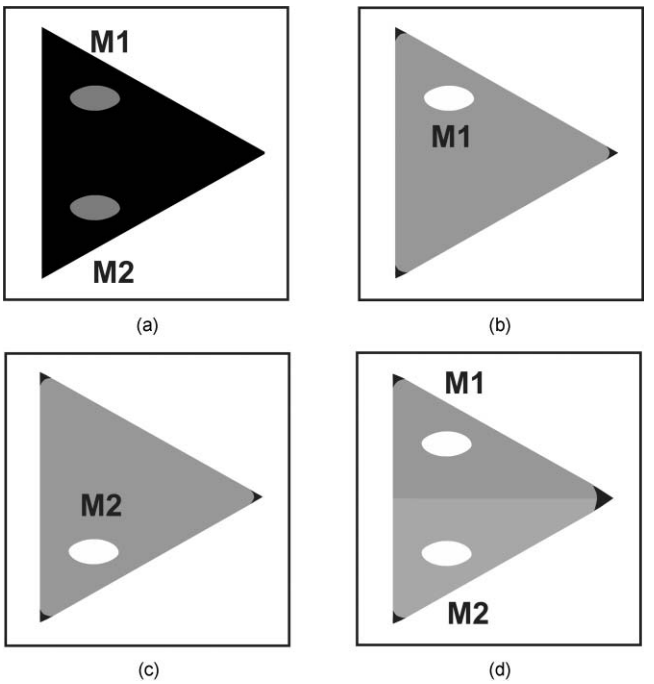

Fig. 3 New influences zones relative to the filtered set: (a) Input set with two markers M_1 and M_2; (b) influence zone of M_1; (c) influence zone of M_2; (d) influence zones of both markers (M_1 or M_2).

The following figures illustrate the computation of $\hat{z}_X(M_i)$. Figure 3(a) displays an input set with two markers M_1 and M_2. Figures 3(b) and 3(c) visualize, respectively, the influence zones of M_1 and M_2, considering that there is only one marker (M_1 or M_2). The shape criterion of the reconstruction has caused that some pixels located at the corners do not belong to the M_1 or M_2 influence zones.

Figure 3(d) shows the influence zones of both markers. Note that there are some (a few) points at the right corner in Fig. 3(d) that do not belong to any influence zones, but that are included in the influence zones in Figs. 3(b) or 3(c). The reason is that there are some pixels that belong to $\hat{\gamma}_{\lambda,g}(X)$ when $g = M_1$ or $g = M_2$, but not when $g = M_1 \bigcup M_2$.

6 Proposed Strategy

This section discusses our proposed strategy to flood labeled markers using a reconstruction criterion for gray-level images. Before that, it is necessary to look through the viscous flooding technique to understand the differences between both approaches.

6.1 *Viscous Watershed*

As mentioned in Sec. 3.3, the topographical relief can be modified to simulate the viscous flooding. To achieve that effect, the relief will be filtered using a morphological closing φ_λ(where λ denotes the structuring element size). Particularly, for simplicity purposes and to facilitate comparisons, it is used a structuring element with the same size in all the flooding stages to modify the relief for all levels, i.e., the viscosity stays invariable in each level.

The gradient to be flooded is the result of the following operation:

$$\varphi^*(f) = \varphi_\lambda[I^*(G(f))], \tag{12}$$

where I^* is the conventional operator to impose minima[45] (if desired), and $G(f)$ is the gradient operator applied to the original image f.

After discussing our strategy in the next section, in Sec. 6.4 we treat the precise differences between the viscous flooding and our approach.

6.2 *Reconstruction with Criterion from Labeled Markers: Gray-Level Case*

The alternative commented in the previous section partially reaches in a certain way the objective stated in Sec. 4. However, it does not solve exactly the problem addressed in this work.

In the following, a strategy that solves the stated problem is discussed. We will apply the concepts commented for the binary case in Sec. 5 to the gray-level case in this section. The input image is considered as a topographical relief that is flooded, as in the standard watershed. We discuss next the expressions of this modified flooding process, which proceeds level by level.

The general schema of the gray-level case of the reconstruction with criterion is displayed in the next pseudocode:

For $h = h_{\min} + 1$ to $h = h_{\max}$

//For all sections at level h to f:

$g = X_{h-1}$

//The set of all catchment basins at level h are computed as follows:

$\hat{z}_A\left(CB_h\left(M_i\right)\right) = \left\{x \in \hat{\gamma}_{\lambda,g}\left(A\right) : D_A\left(x, \left(CB_h\left(M_i\right)\right)\right)\right.$

$\left.\text{finite}, \forall j \neq i,\ D_A(x, (CB_h(M_i))) < D_A(x, (CB_h(M_j)))\right\}$

$X_h = \hat{z}_A(CB_h(M_i))$

$h = h + 1$

Let $h_{\min}$($h_{\max}$, respectively) be the smallest value (greatest value, respectively) of the gray-scale input image f within its domain D_f. Let $CB\,(M)$be the basin associated with minimum M, and $CB_h\,(M)$ the set of all the points of the basin that have an altitude less than or equal to h, that is,

$$\begin{aligned} CB_h(M) &= \{p \in CB(M) | f(p) \leq h\} \\ &= CB(M) \cap T_h(f), \end{aligned} \tag{13}$$

where $T_h\,(f)$ denotes a thresholding transformation, with a threshold value equal to h.

Consider now X_h the subset of all basins with a gray-scale value less than or equal to h:

$$X_h = \cup_i CB_h(M_i). \tag{14}$$

The influence zones relative to the filtered set, as well as how to compute them, are introduced in Sec. 5. According to those previous definitions, we consider the catchment basins associated to the M_i markers set for each level section in the gray-level case. That is, each level is treated separately, and the influence zones for each catchment basin are considered in a similar manner to the binary case:

$$\begin{aligned} &\hat{z}_A[CB_h(M_i)] = \{x \in \hat{\gamma}_{\lambda,g}(A) : D_A\{x, [CB_h(M_i)]\}\ \text{finite}, \\ &\forall j \neq i,\ D_A\{x, [CB_h(M_i)]\} < D_A\{x, [CB_h(M_j)]\}, \end{aligned} \tag{15}$$

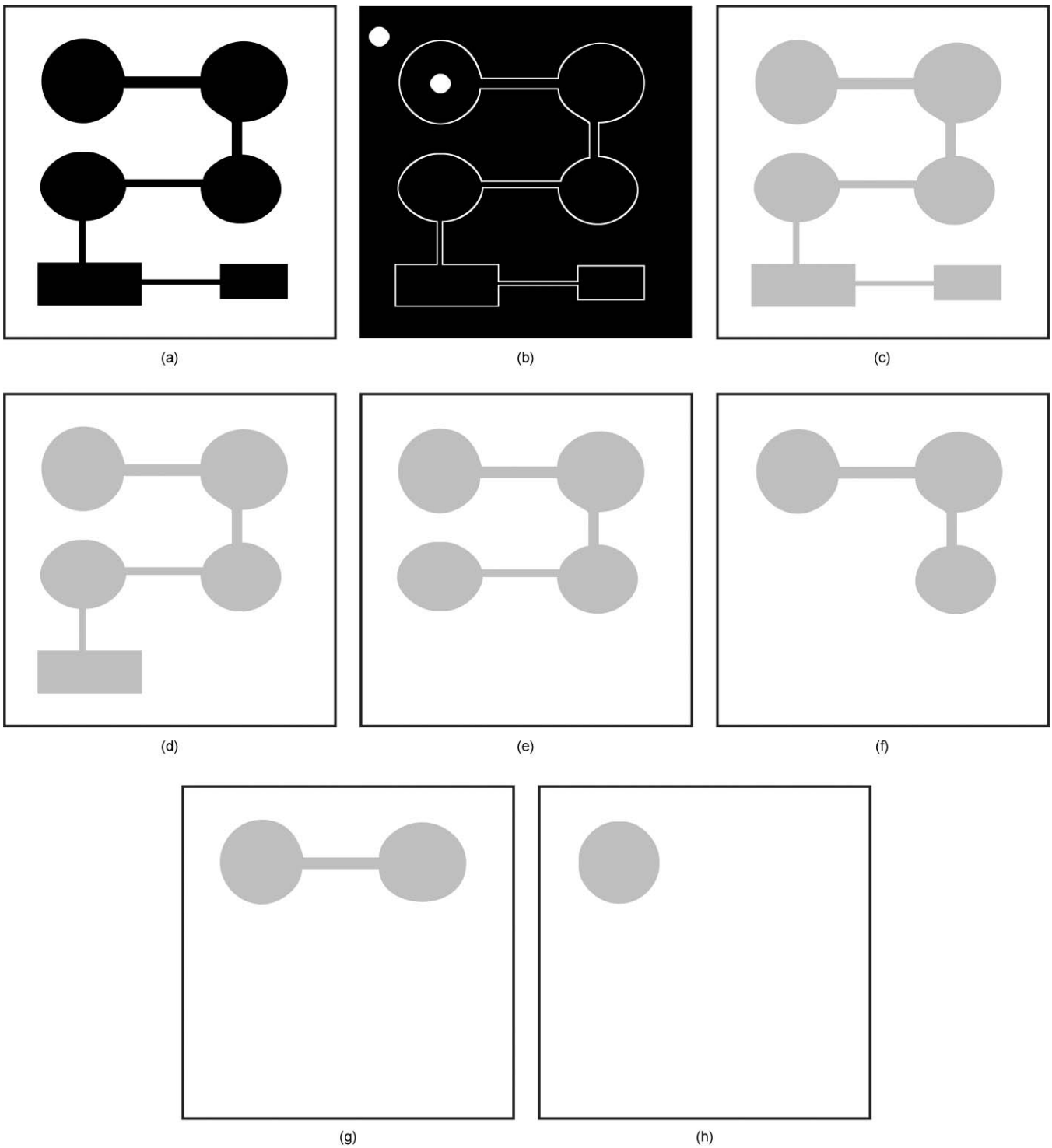

Fig. 4 (a) Original image; (b) gradient operator over the original image (markers are high-lighted in white); (c) result of a standard watershed (Beucher-Meyer's method); (d) result of a modified flooding with γ_λ, where λ=1; (e) the same, where λ=2; (f) the same, where λ=3; (g) the same, where λ=4; and (h) the same, where λ=5.

where $g = \bigcup_i CB_h(M_i) = X_h$ and A is a mask level defined as

$$A = \mathrm{MASK}_h(f) = \begin{cases} \mathrm{MAX\,VALUE} & \forall x : f(x) \leq h \\ 0 & \text{otherwise,} \end{cases} \quad (16)$$

Here MAX VALUE represents the maximum value of the images under consideration. (For unsigned 2 byte/pixel images, MAX VALUE is equal to 65,535).

The $X_{h_{\min}}$ initial marker is composed of the set of all regional minima of the input image f. The basins will be

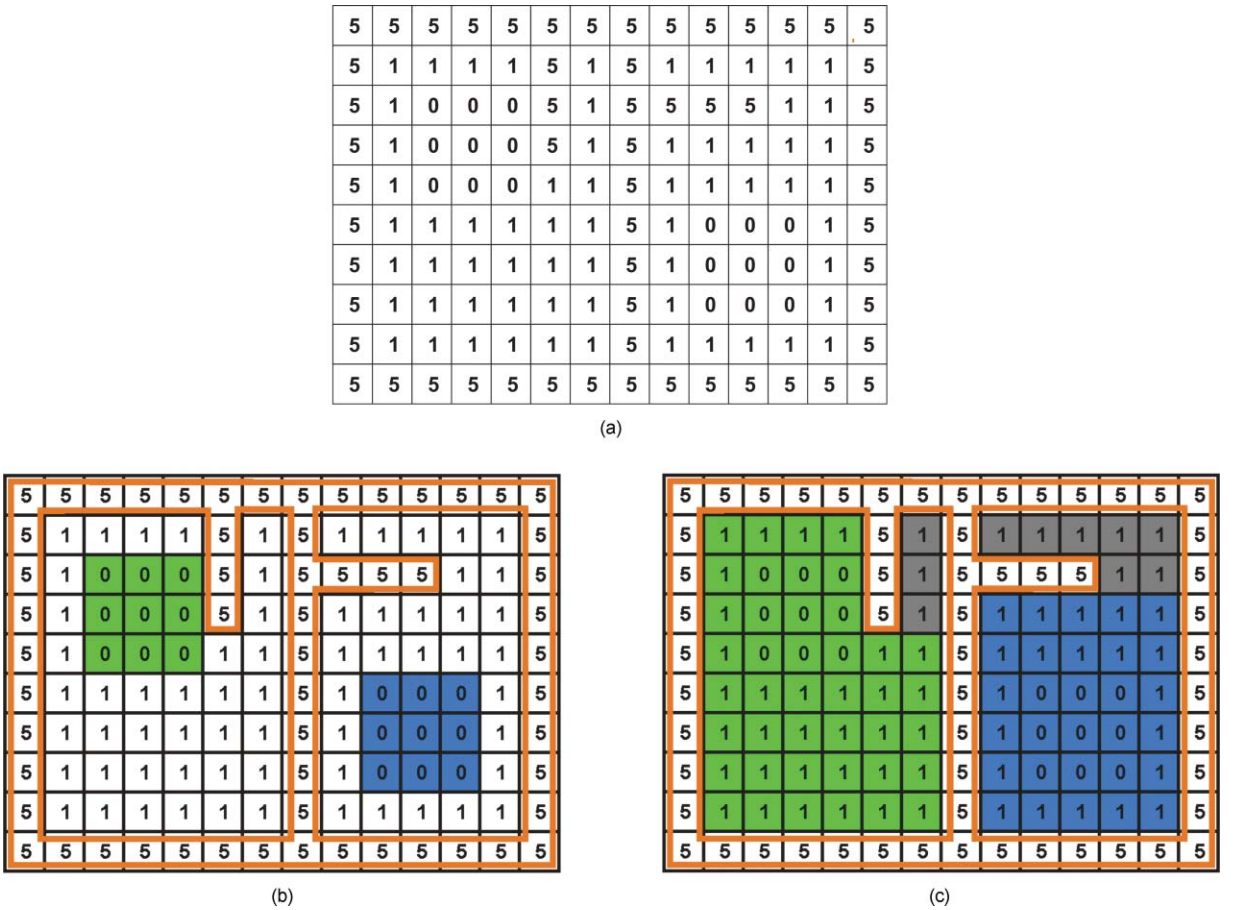

Fig. 5 (a) Gradient image; (b) mask at level 1 with initial markers highlighted; and (c) result of both a viscous flooding and our proposed modified flooding with γ_λ, where λ=1.

progressively formed by a modified flooding process that starts at the minima $X_{h_{\min}}$. In addition, the modified flooding remains within the limits imposed by the mask at level i. We take the new $\hat{z}_A[CB_h(M_i)]$ influence zones of markers M_i at each level h as the new markers set for the next $h+1$ level $[CB_{h+1}(M_i)]$.

At the end of the process, the watershed lines are the frontiers of the catchment basins. Note that some pixels can be left unflooded (as discussed in Sec. 5 for the binary case) because of the added reconstruction criterion. The γ_λ criterion that is introduced provides the flexibility to control and to limit the reconstruction process in certain areas.

6.3 *Some Results*

In the following, we experiment with a basic 3×3 square structuring element for all the figures, but other types of structuring elements can be used in order to obtain different results in the final shapes recovered.

Figure 4 illustrates the effect of changing the criterion. Figure 4(a) is the input image, and Fig. 4(b) shows its image gradient, where the markers are displayed as white circles, one inside the region and another one outside (in the background). Figure 4(c) shows the result of a standard watershed (Beucher-Meyer's method[14]). Five results of applying the modified flooding process using different reconstruction criteria (increasing the size of the structuring element in each case) are shown in Figs. 4(d), 4(e), 4(f), 4(g), and 4(h).

As can be observed, the added criterion controls the propagation of the initial marker through the thin zones that connect each circle. The larger the structuring element of the added criterion, the more the reconstruction is restricted.

6.4 *Comparison of the Proposed Modified Flooding and the Viscous Watershed*

This section compares the differences between our strategy and the viscous watershed. As mentioned in Sec.3.3, the viscous watershed modifies the surface (the gradient) to be flooded by applying a filter (a morphological closing). Such a filter can vary depending on the level to simulate the behavior of the viscous fluid.

Our proposed strategy, however, modifies the flooding process itself by using a morphological opening that constrains the propagation of each labeled marker. This way, the flooding is prevented to proceed into certain parts.

The contours of the catchment basins computed by the viscous watershed and by our strategy can differ; the larger the number of markers that are propagating at a certain level, the larger the differences will become. In addition, the possibility exists that certain pixels are left unflooded in our strategy, since ensuring the desired shape criteria is paramount. Two

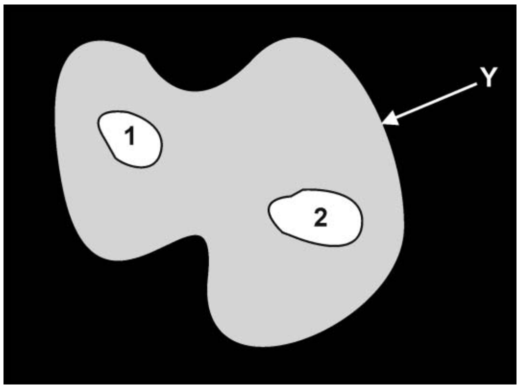

Fig. 6 Case with two propagating markers inside a mask Y at a certain level.

situations can be distinguished, depending on the number of markers that are present at each mask level:

1. The evolutions of the flooding by our strategy and that by the viscous watershed are the same if there is only one marker per connected component (at each level). See Fig. 5.
2. On the other hand, the evolution could be different between the two processes, when a connected component of the mask to be flooded at a certain level contains more than one propagating marker from the previous level. This type of situation is shown in Fig. 6. (In the normal watershed method, the catchment basins associated to the contained markers can be obtained in this case by computing the geodesic influence zones of the markers within the mask.)

For the first case, an example is shown in Fig. 5. In this image, we have two different markers (with value 0), each one in a separate connected component at level 1. Note that there is other connected component at level 5, which are highlighted with a bright tone; this zone is not considered for flooding in the test. Those pixels that cannot be flooded (because the restriction imposed by the viscous closing or by the reconstruction criterion) are displayed in dark tone in Fig. 5(c). In this case, there are not differences between the viscous watershed and our approach.

The second case is illustrated in the example of Fig. 7. In this image, there exist three markers (with value 0) in one connected component at level 1, which are highlighted with different tones in Fig. 8(a).

In the same way, those pixels at level 5 (highlighted with a bright tone) are not considered in the selected stage. In the case of the viscous watershed, the flooding scenario is modified by applying a morphological closing of size λ=2. This is shown in Fig. 8(a), where the pixels signaled by an arrow are those that will be eliminated from the flooding scenario in the mask at level 1 [see Fig. 8(b)]. After this operation is realized, a normal flooding process without restrictions (like that performed by a standard watershed algorithm) is performed. As a consequence of this, all the markers are flooded to the same rate, and they met in the intermediate point [Fig. 8(d)]. The viscous flooding computes the result displayed in Fig. 8(e).

5	5	5	5	5	1	0	0	0	0	1	5	5	5	5	5
5	5	5	5	5	1	0	0	0	0	1	5	5	5	5	5
5	5	5	5	5	1	0	0	0	0	1	5	5	5	5	5
5	5	5	5	5	1	1	1	1	1	1	5	5	5	5	5
5	5	5	5	5	1	1	1	1	1	1	5	5	5	5	5
5	5	5	5	5	1	1	1	1	1	1	5	5	5	5	5
5	5	5	5	5	1	1	1	1	1	1	5	5	5	5	5
5	5	5	5	5	1	1	1	1	1	1	5	5	5	5	5
5	5	5	5	5	1	1	1	1	1	1	5	5	5	5	5
5	5	5	5	5	1	1	1	1	1	1	5	5	5	5	5
5	5	5	5	5	1	1	1	1	1	1	5	5	5	5	5
5	5	5	5	5	1	1	1	1	1	1	5	5	5	5	5
5	5	1	1	1	1	1	1	1	1	1	1	1	1	5	5
5	5	1	1	1	1	1	1	1	1	1	1	1	5	5	5
5	5	5	5	5	1	1	1	1	1	1	5	5	5	5	5
1	1	1	1	1	1	1	1	1	1	1	1	1	1	1	1
1	0	0	0	0	1	1	1	1	1	1	0	0	0	0	1
1	0	0	0	0	1	1	1	1	1	1	0	0	0	0	1
1	0	0	0	0	1	1	1	1	1	1	0	0	0	0	1
1	1	1	1	1	1	1	1	1	1	1	1	1	1	1	1

Fig. 7 Gradient image used in the comparison of Figs. 8 and 9.

At first, it could be thought that the flooding evolution would be the same using our proposed flooding strategy, because all regions eliminated from the flooding scenario by the viscous watershed (by applying the closing) would not be flooded by any of the markers since the flooding is restricted by the opening. (The structuring element size of the opening is λ=2, which corresponds to the size of the morphological closing used in the previous figure.) However, we must consider that the idea proposed in this paper implies the restriction of the flooding of each marker separately. This fact causes differences with the viscous flooding that can be observed when the proposed strategy is applied to the case of Fig. 7. When the restriction affects each marker separately, the propagation of the two markers located at the lower part cannot continue once the central corners are reached [Figs. 9(c) and 9(e)], because the individual restriction imposed by the criterion of each marker. Therefore, the propagation of the marker at the upper part will eventually flood and label more pixels located at the central part [Fig. 9(g)]; in this way, this marker will finish flooding all the region [Fig. 9(h)].

We use the image visualized in Fig. 10 to compare the differences between the viscous watershed and our proposed modified flooding with several criteria values in Fig. 11. There are some differences in the watershed lines obtained by the two methods. Another less evident difference, is the existence of some pixels that could not be flooded or recovered in the final image (pixels left unflooded have black color in Fig. 11). The number of unflooded pixels is variable and depends on the size of the structuring element. Note that the differences between the images occurs in those

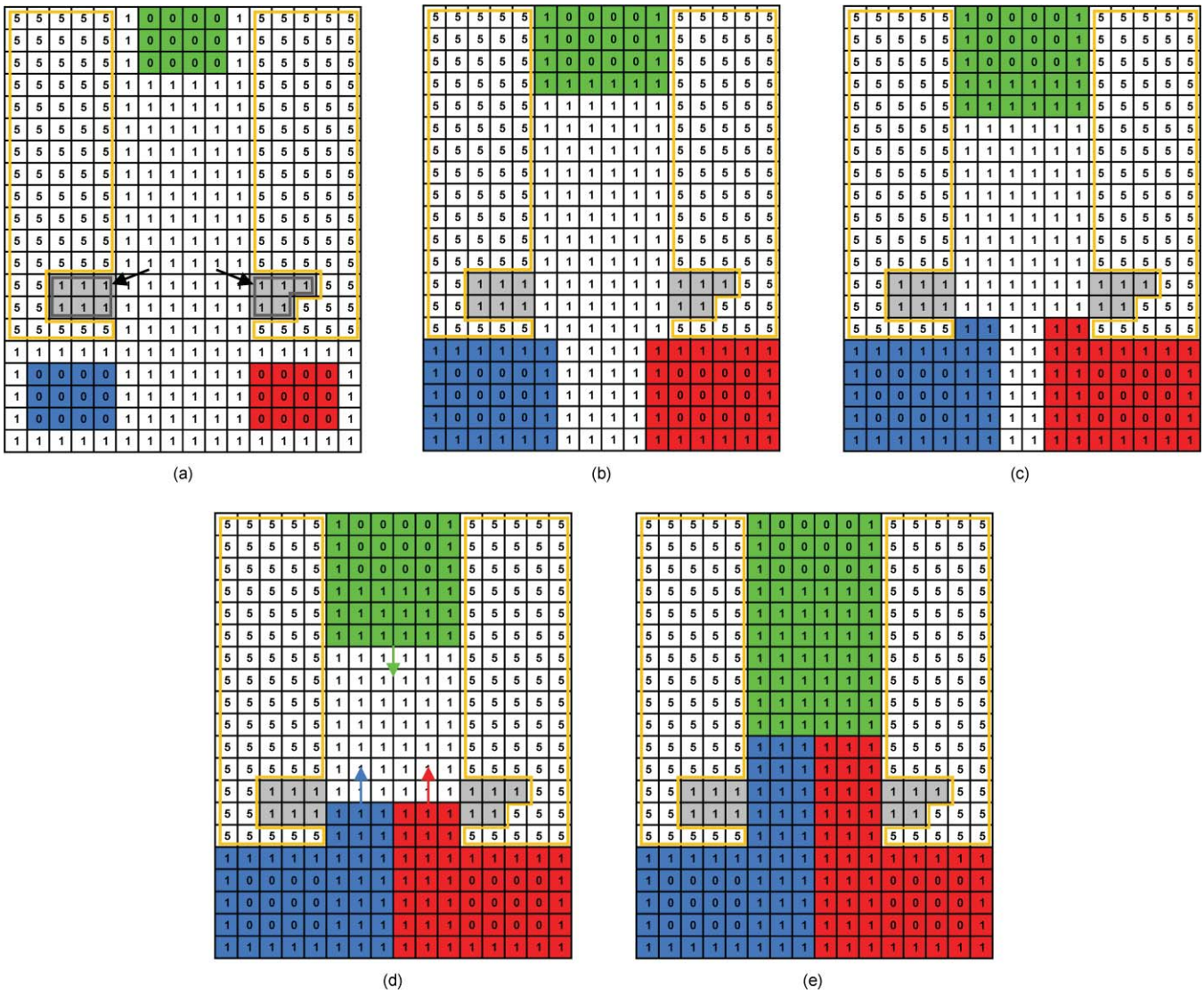

Fig. 8 Comparative between the viscous watershed and the proposed strategy (part A): (a) Initial flooding scenario at level 1 (markers are highlighted with different tones); (b), (c), (d), and (e) shows progressive evolution of the viscous watershed using φ_λ (where $\lambda = 2$) to modify the gradient.

positions where different markers have joined, changing the final forms because the viscosities coming from more than a source interact.

As we can observe in the provided examples, the viscous watershed does not strictly fulfills the shape criterion in all situations. When imposing the criterion in the flooding scenario by using a closing, it is forced a unique viscosity for the entire image, limiting the flexibility of the process. By considering the criterion restriction to each marker separately, our method guarantees the shape criterion.

In this way, if an opening is applied to any one of the final regions of the segmentation using the cited shape criterion, they do not change (they are invariant). In the case of the viscous watershed, this situation does not always happens (as can be observed in the comparative of the internal regions in Fig. 10).

As mentioned, the viscous watershed and our approach share some similarities; particularly when only one marker is present in the flooding scenario, both methods work in the same manner. We can take advantage of this situation to optimize the algorithm by, first until two or more markers meet in the scenario, using the viscous closing to modify the scenario and employ a conventional flooding, and when markers have met, switching to the method proposed. In this way, the execution time of the algorithm is reduced.

7 Experimental Results

We mainly used the biomedical domain to experiment with our proposed technique. Two medical images have been selected for comparison in Figs. 12 (354×400 pixels) and 13 (750×576 pixels). In the first line of these figures the original image [part (a)] and the result of a standard watershed [part (b)] are displayed; in the second line, we show the results of a viscous watershed using different sizes of structuring element**;** finally, in the third line the results of our technique using the proposed modified gradient flooding with different criteria $\gamma_\lambda$are displayed.

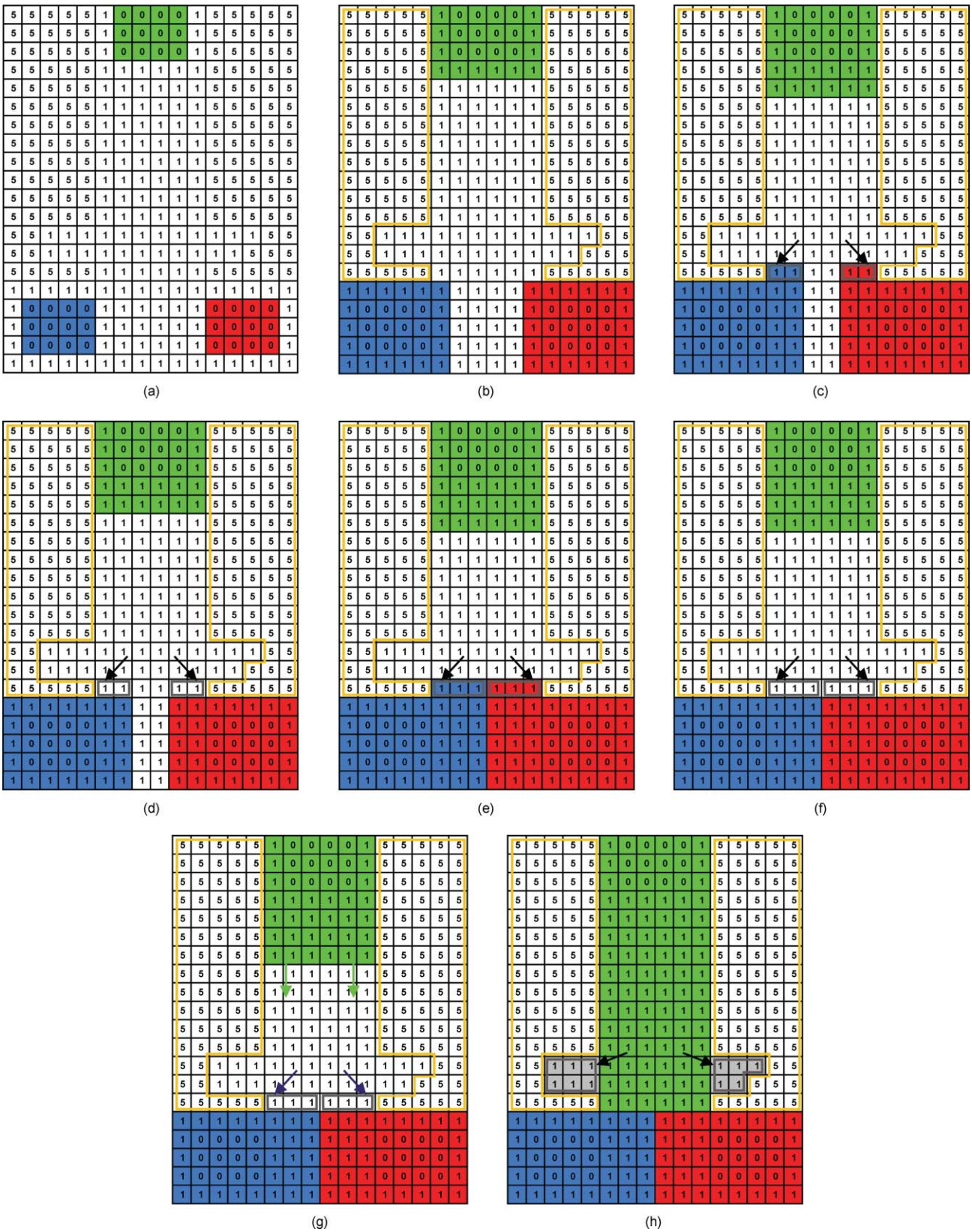

Fig. 9 Comparative between the viscous watershed and the proposed strategy (part B): (a) Initial flooding scenario at level 1 (markers are highlighted with different tones); (b), (c), (d), (e), (f), (g), and (h) shows progressive evolution of the proposed flooding whit criterion γ_λ, where $\lambda = 2$.

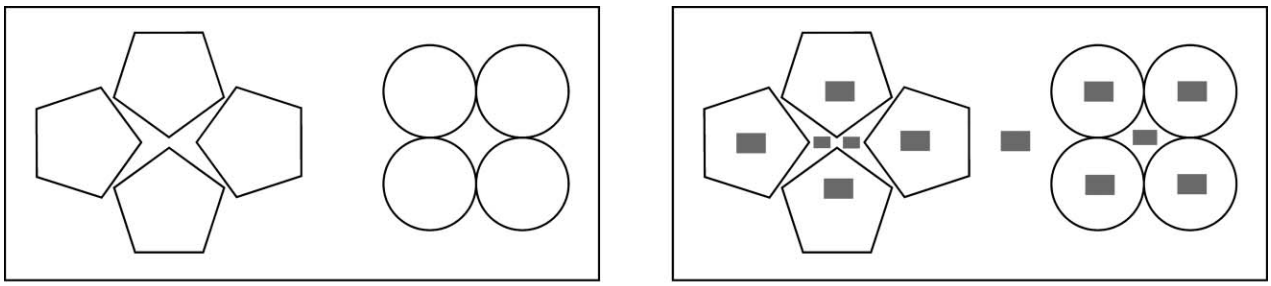

Fig. 10 (a) Original image, (b) result of a standard watershed. The maskers are indicated in gray tone (the background has its own marker).

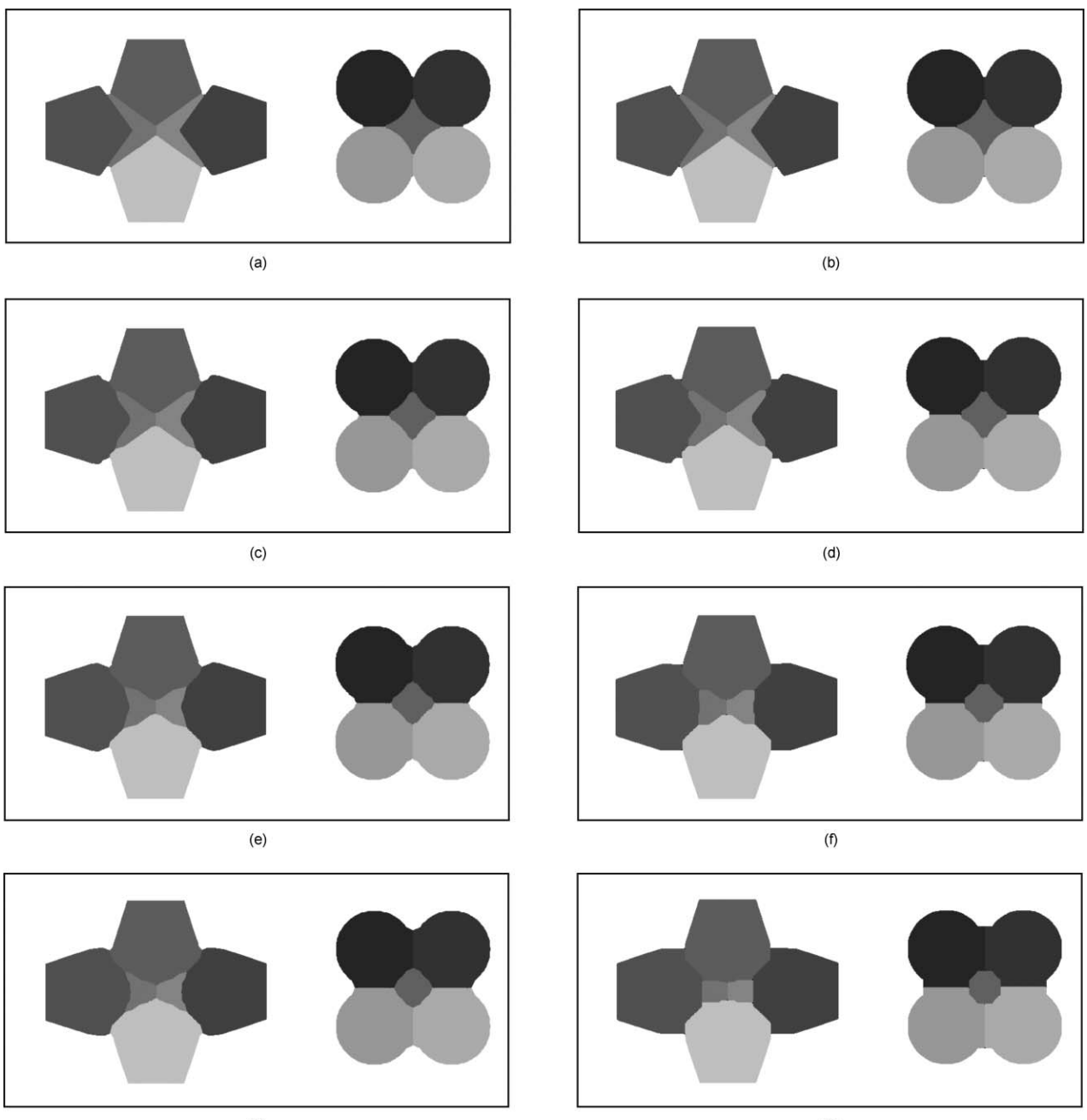

Fig. 11 Comparison between the viscous watershed and the proposed flooding strategy using several structuring elements (λ=1, 4, 7, 10). (a), (b), (c), and (d) correspond with the viscous watershed algorithm; (e), (f), (g), and (h) correspond with our approach.

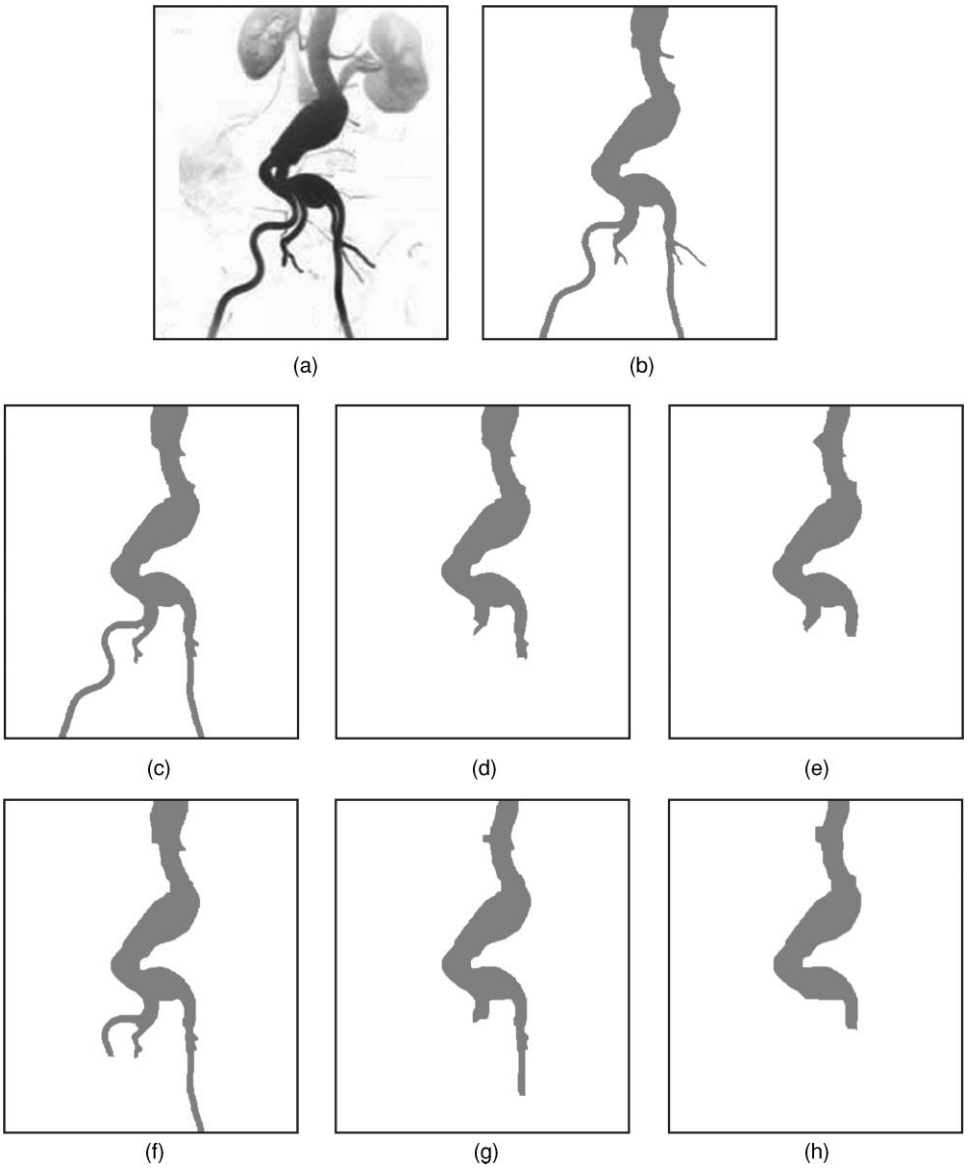

Fig. 12 (a) Original image[46]; (b) result of a standard watershed (Beucher-Meyer's algorithm); (c) the result of a viscous watershed using λ=1, (d) λ=2, and (e) λ=4. Result of our modified gradient flooding with γ_λ, where (f) λ=1, (g) λ=2, and (h) λ=4.

The execution times have been as follows. In Fig. 12, using λ=1 the proposed algorithm takes 3 s to perform the operation; with λ=2 the time is less than 4 s; and the algorithm takes 4 s employing λ=4.

In the Fig. 13 case, the algorithm needs more time to perform the operation: for λ=1, the algorithm takes 18 s, and for λ=2 the time employed was 21 s. A PC Core 2 Duo 2.2 GHZ with 4 GBytes RAM (under Windows XP, with compiler Builder C 6.0) was used.

Note that the major size of the image is not the principal cause of the time delay, but the initial size of the markers and its position inside the image. The principal factor that increases the execution time of the algorithm is mainly the interaction among the viscosities of different markers in a specific flooding scenario.

Depending on the structuring element size, using our proposed method we can control how the regions of interest are extracted. By increasing the size criterion, it is possible to restrict the segmentation process so that the flooding does not propagate to certain thin structures.

8 Conclusions

A new segmentation method based on the watershed approach that incorporates a shape criterion was proposed. Particularly, the presented technique is a gradient flooding method that constrains how the flooding proceeds and, as a consequence, can control the characteristics of the shapes of the extracted regions.

The proposed technique extends a shape criterion that had been used in some filters (the filters with reconstruction criterion) into the segmentation stage. The shape criterion is imposed by means of incorporating an opening that limits each propagation step (an adapted geodesic dilation) of the labeled markers.

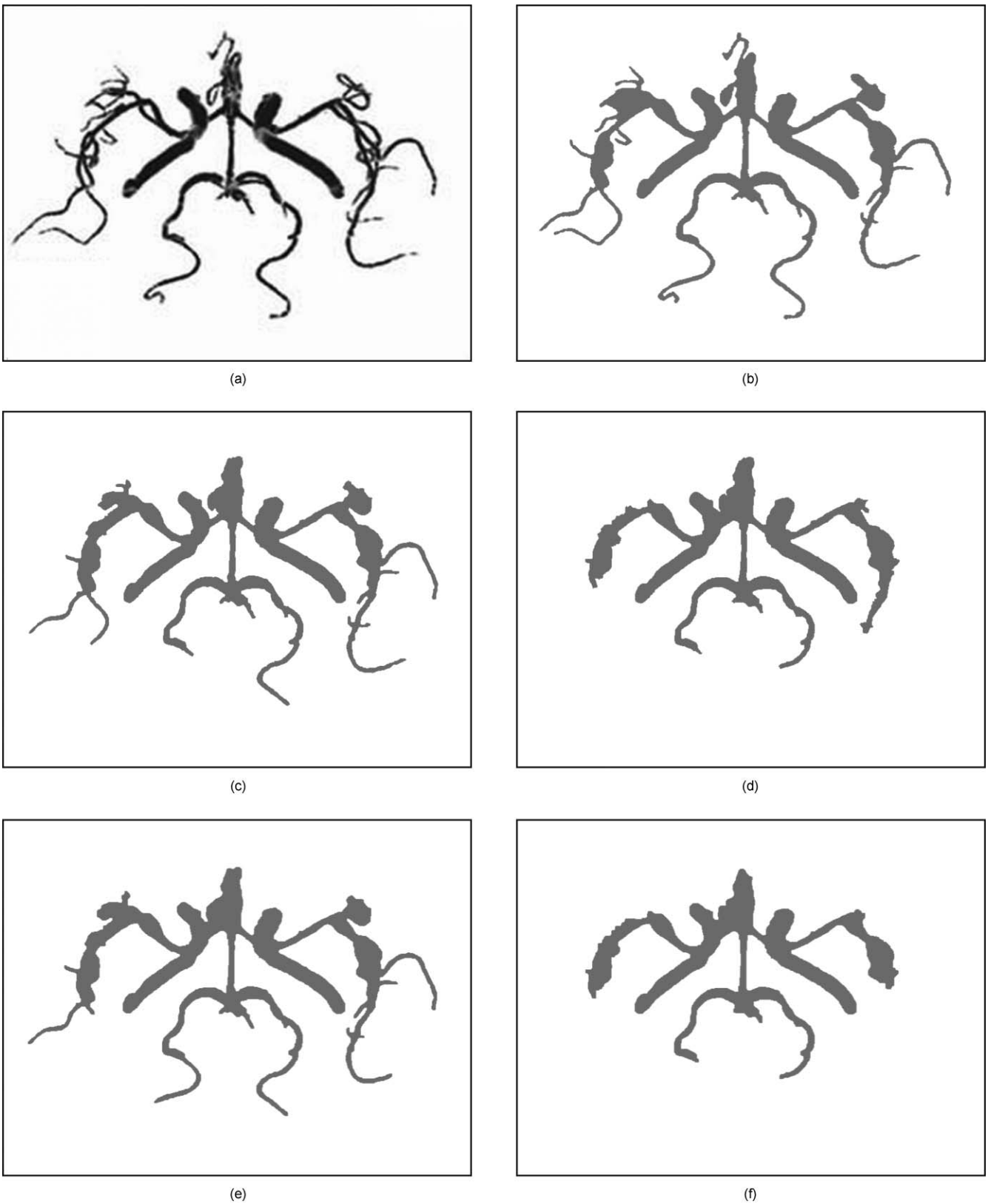

Fig. 13 (a) Original image[46]; (b) result of a standard watershed (Beucher-Meyer's algorithm); (c) result of a viscous watershed using λ=1 and (d) λ=2. Result of our modified gradient flooding with γ_λ, where (e) λ=1 and (f) λ=2.

We also commented on the relationship with other watershed variant such as the viscous watershed. Some experimental results were provided using, especially, the biomedical domain. This domain is particularly well suited for a technique such as ours that provides greater flexibility and control in the extraction of particles and structures. Nevertheless, the proposed technique can generally be applied to any type of domain.

As mentioned, the shape constraints of the proposed method can cause some pixels (usually, a very small number) to be left unassigned. In many applications, this is not normally a major issue (such as, for example, in particle extraction applications), and it is a direct consequence of imposing the desired shape constraints. In cases where this could be an issue, those pixels can be assigned in a final step, although this would obviously cause the shape constraints to be unsatisfied.

We must take into account that last fact. Because of the fact that some pixels can be left unflooded, technically our proposal is not a "traditional" image segmentation.

This method does not always generate a total partition of the image definition domain, because some pixels (those that have been left unflooded) may not be allocated to any of the input markers. For this reason, this approach generates a "partial" segmentation of the entire domain. In future work, we intend to go deeply into this subject and possibly suggest modifications in the original method for new results and applications.

Acknowledgments

This work has been supported in part by the "Fondo Sectorial de Investigación para la Educación" (SEP-CONACyT 2007-México), by the "Universidad Politécnica de Madrid," and by "Ministerio de Ciencia e Innovación" of Spain TIN2007-61768.

References

1. R. C. Gonzalez and R. E. Woods, *Digital Image Processing*, 3rd ed., Pearson Education-Prentice Hall, Upper Saddle River, NJ (2008).
2. J. Bernd, *Digital Image Processing*, Springer-Berlin Heidelberg, New York (2005).
3. G. Matheron, *Random Sets and Integral Geometry*, Wiley, New York (1975).
4. J. Serra, *Mathematical Morphology*, Vol. I, Academic Press, London (1982).
5. J. Serra, *Mathematical Morphology, Volume II: Theoretical Advances*, Academic Press, London (1988).
6. C. Giardina and E. Dougherty, *Morphological Methods in Image and Signal Processing*, Prentice-Hall, Englewood Clliffs, NJ (1988).
7. M. Schmitt and J. Mattioli, *Morphologie Mathématique*, Masson, Paris (1993).
8. H. Heijmans, "Morphological image operators," in *Advances in Electronics and Electron Physics*, P. Hawkes, series Ed., Academic Press, Boston (1994).
9. P. Soille, *Morphological Image Analysis: Principle and Applications*, Springer-Verlag, Berlin, Heidelberg, New York (1999).
10. E. Dougherty and R. Lotufo, *Hands-on Morphological Image Processing*, SPIE Optical Engineering Press, Bellingham, WA (2003).
11. S. Beucher and C. Lantuéjoul, "Use of watersheds in contour detection," in *Proc. Int. Workshop on Image Processing*, pp. 17–21 (1979).
12. S. Beucher, "Segmentation d'images et morphologie mathématique," PhD thesis, E. N. S. des Mines de Paris (1990).
13. L. Vincent and P. Soille, "Watersheds in digital spaces: an efficient algorithm based on immersion simulations," *IEEE Trans. Pattern Anal. Mach. Intell.* **13**(6), 583–598 (1991).
14. S. Beucher and F. Meyer, "The morphological approach to segmentation: the watershed transformation," Chap. 12 in *Mathematical Morphology in Image Processing*, E. Dougherty, Ed., pp. 433–481, Marcel Dekker, New York (1993).
15. L. Najman and M. Schmitt, "Geodesic saliency of watershed contours and hierarchical segmentation," *IEEE Trans. Pattern Anal. Mach. Intell.* **18**(12), 1163–1173 (1996).
16. R. Adams and L. Bischof, "Seeded region growing," *IEEE Trans. Pattern Anal. Mach. Intell.* **16**(6), 641–647 (1994).
17. J. Crespo, R. Schafer, J. Serra, C. Gratin, and F. Meyer, "The flat zone approach: a general low-level region merging segmentation method," *Signal Process.* **62**(1), 37–60 (1997).
18. D. Brunner and P. Soille, "Iterative area seeded region growing for multichannel image simplification," in *Computational Imaging and Vision*, C. Ronse, L. Najman, and E. Decenciere, Eds., Vol. 30, pp. 397–406, Springer-Verlag, Dordrecht (2005).
19. D. Brunner and P. Soille, "Iterative area filtering of multichannel images," *J. Image Vis. Comput.* **25**, 1352–1364 (2007).
20. G. Bertrand, "On topological watersheds," *J. Math. Imaging Vis.* **22**(2–3), 217–230 (2005).
21. H. Nguyen, M. Worring, and R. van den Boomgaard, "Watersnakes: energy driven watershed segmentation," *IEEE Trans. Pattern Anal. Mach. Intell.* **25**(3), 330–342 (2003).
22. F. Meyer, "Inondation par des fluids," Technical Report Note Interne CMM, Ecole des Mines de Paris (1993).
23. J. Serra and P. Salembier, "Connected operators and pyramids," in *Non-Linear Algebra and Morphological Image Processing*, *Proc. SPIE* **2030**, 65–76 (1993).
24. J. Crespo, J. Serra and R. Schafer, "Image segmentation using connected filters," in *Proc. Int. Workshop on mathematical morphology and its Applications to Signal Processing*, J. Serra, and P. Salembier, Eds., pp. 52–57 (1993).
25. L. Vincent, "Morphological grayscale reconstruction in image analysis: Applications and efficient algorithms," *IEEE Trans. Image Process.* **2**, 176–201 (1993).
26. P. Salembier and J. Serra, "Flat zones filtering, connected operators, and filters by reconstruction," *IEEE Trans. Image Process.* **4**(8), 1153–1160 (1995).
27. J. Crespo, J. Serra, and R. Schafer, "Theoretical aspects of morphological filters by reconstruction," *Signal Process.* **47**(2), 201–225 (1995).
28. J. Crespo and R. Schafer, "Locality and adjacency stability constraints for morphological connected operators," *J. Math. Imaging Vis.* **7**(1), 85–102 (1997).
29. J. Crespo and V. Maojo, "New results on the theory of morphological filters by reconstruction," *Pattern Recog.* **31**(4), 419–429 (1998).
30. E. J. Breen and R. Jones, "Attribute openings, thinnings and granulometries," *Comput. Vis. Image Understand.* **64**(3), 337–389 (1996).
31. D. Vargas, J. Crespo, and V. Maojo, "Morphological image reconstruction with criterion from labelled markers," in *Discrete Geometry for Computer Imagery*, *Lecture Notes in Computer Science* **2886**, 475–484 (2003).
32. D. Vargas, "*Filtros morfologicos conexos: deteccion de cisuras en imagenes obtenidas por resonancia magnetica del cerebro*," Master's thesis, Universidad Autonoma de Queretaro, Mexico (2000).
33. D. Vargas and I. Terol, "Transformaciones por reconstruccion con criterios de propagacion: una nueva clase de filtros morfológicos," in *Proc. Int. Conf. on Artificial Intelligence MICAI*, pp. 117–126 (2000).
34. I. R. Terol and D. Vargas, "Openings and closings by reconstruction using propagation criteria," in *Computer Analysis of Images and Patterns*, *Lecture Notes in Computer Science* **2124**, 502–509 (2001).
35. I. R. Terol and D. Vargas, "A study of openings and closings with reconstruction criteria," in *Mathematical Morphology, Proc. VIth Int. Symp.*, H. Talbot and R. Beare, Eds., pp. 413–423, CSIRO Publishing, (2002).
36. D. Vargas, J. Crespo, V. Maojo, and I. Terol, "Medical image segmentation using openings and closings with reconstruction criteria," in *Proc. Int. Conf. on Image Processing ICIP*, Vol. 3, pp. 981–984 (2003).
37. I. R. Terol and D. Vargas-Vazquez, "Openings and closings with reconstruction criteria: a study of a class of lower and upper leveling," *J. Electron. Imaging* **14**(1), 013006 (2005).
38. J. Rivest, P. Soille, and S. Beucher, "Morphological gradients," *J. Electron. Imaging* **2**(4), 326–336 (1993).
39. G. Matheron, *Éléments pour une Théorie des Milieux Poreux*, Masson, Paris (1965).
40. P. Salembier, "Morphological multiscale segmentation for image coding," *Signal Process.* **38**(3), 359–386 (1994).
41. J. Serra, "Viscous lattices," in *Proc. Int. Symp. ISMM*, pp. 79–90 (2002).
42. F. Meyer and C. Vachier, "Image segmentation based on viscous flooding simulation," in *Proc. Int. Symp. ISMM*, pp. 69–77 (2002).
43. C. Vachier and F. Meyer, "The viscous watershed transform," *J. Math. Imaging Vis.* **22**(2–3), 251–267 (2005).
44. C. Vachier and F. Meyer, "News from viscousland," in *Proc. 8th Int. Symp. ISMM*, pp. 189–200 (2007).
45. P. Soille, *Morphological Image Analysis: Principles and Applications*, 2nd ed., Springer-Verlag, Berlin, Heidelberg, New York (2003).
46. O. R. Tenreiro, http://www.cirugiaendovascular.com.ve/index.htm., website: endovascular surgery (2007).

Damián Vargas-Vázquez received his diploma in electronic engineering from the Instituto Tecnológico de Querétaro, Mexico, in 1995, his MS degree in instrumentation and automatic control from the Universidad Autónoma de Querétaro, Mexico, in 2000, and his PhD degree in computer science from the Universidad Politécnica de Madrid, Spain, in 2007. In 2007 he joined the School of Engineering, the Universidad Autónoma de Querétaro, Mexico, where he is currently a research professor in the image processing and analysis field, particularly in illumination and mathematical morphology.

Jose Crespo received his diploma as "Ingeniero de Telecomunicación" from the Universidad Politécnica de Madrid in 1989. From the Georgia Institute of Technology, he received his MS degree in electrical engineering in 1990, his MS degree in management in 1993, his PhD degree in electrical and computer engineering in 1993, and his PhD degree in computer science in 2006. He has been a postdoctoral researcher with the Centre de Morphologie Mathématique (E.N.S. des Mines de Paris), an associate professor with the Universidad Alfonso X el Sabio, and in 1995, he joined the School of Computer Science, the Universidad Politécnica de Madrid, where he is currently an associate professor and heads the LSIIS Department. His main research interests are image processing and analysis, mathematical morphology, biomedical imaging, biomedical informatics, and e-learning.

Victor Maojo received his MD degree from the University of Oviedo, Spain, in 1985 and his PhD degree in computer science from the Universidad Politecnica de Madrid (UPM) in 1990. At the UPM, he is currently a full professor and director of the Biomedical Informatics Group. Before entering the faculty of the UPM, he was a postdoctoral researcher and consultant with Georgia Tech, Atlanta, from 1990 to 1991 and a research fellow with the Decision Systems Group, Harvard University-Massachusetts Institute of Technology (MIT), Boston, from 1991 to 1993). He has been the principal investigator on more than 20 national and international projects and has authored more than 100 scientific papers and books. He has been a member of numerous committees at international conferences and journals and was as an expert for the IV, V, VI, and VII Framework Programmes of the European Commission.

Jose Gabriel Ríos-Moreno received his BS and MS degrees in automatic control in the Facultad de Ingeniería, in 2003 and 2005, respectively, and his PhD in intelligent buildings in 2008 all from the Universidad Autónoma de Querétaro, Mexico, where he is currently a Professor with the School of Engineering. His research interests include image processing, thermal modeling, and automatic illumination control for intelligent buildings.

Mario Trejo-Perea received his BS and MS degrees in automatic control and his PhD degree from the Universidad Autónoma de Querétaro, Mexico, in 1994, 2005, and 2008, respectively. He has published some scientific papers in journals and presented papers at conferences on energy consumption prediction using neural networks models. In 1994 he joined the School of Engineering, the Universidad Autónoma de Querétaro, Mexico, where he is a research professor. His main research interests are signal processing and the development of models predicting load in intelligent buildings.